05

Peculiarities of deformation of round thin-film membranes and experimental determination of their effective characteristics

© A.A. Dedkova,[1] P.Yu. Glagolev,[1] E.E. Gusev,[1] N.A. Dyuzhev,[1] V.Yu. Kireev,[1] S.A. Lychev,[2] D.A. Tovarnov[1]

[1] National Research University of Electronic Technology,
124498 Zelenograd, Moscow, Russia
[2] Ishlinsky Institute for Problems in Mechanics, Russian Academy of Sciences,
119526 Moscow, Russia
e-mail: dedkova@ckp-miet.ru

Received April 26, 2021
Revised April 26, 2021
Accepted April 26, 2021

The features of thin-film membranes, which are formed above round holes in silicon substrates using the Bosch-process are considered. The membrane has a complex shape due to the presence of the stress state of the initial films. The analysis of the dependence of the membrane deflection w on the supplied overpressure P is used to calculate the mechanical characteristics of the membranes. In this case, it is necessary to determine directly on the membrane its diameter, the thickness of the constituent layers, the change in the topography of the membrane surface over its entire area as the overpressure increases. Determination of the membrane diameter and the thicknesses of the constituent layers is shown by the example of p-$Si^*/SiN_x/SiO_2$ and $SiN_x/SiO_2/SiN_x/SiO_2$ membranes. We used spectral ellipsometry, energy-dispersive X-ray spectroscopy, optical profilometry, optical microscopy. The influence of the peculiarities of the fixing conditions on the stress-strain state of membranes is shown, and the assessment is carried out by means of numerical modeling. A technique has been developed for measuring and calculating the mechanical characteristics of membranes that have an initial deflection. The calculation result is shown on the example of a membrane with an initial deflection of $2\,\mu$m — $SiN_x/SiO_2/SiN_x/SiO_2$ and a membrane with an initial deflection of $30\,\mu$m — $Al/SiO_2/Al$.

Keywords: stress, bulging method, films, thin-layer coating, film thickness, membrane, pressure blister test, residual stress, microelectromechanical systems, MEMS, silicon substrate, large deformations, strain, deflections, circular membrane, bulge testing.

DOI: 10.21883/TP.2022.13.52218.121-21

Introduction

Currently the special attention is given to the issues of analysis of a stress-strain state, appearing in microelectromechanical systems (MEMS). Study objects are circular membranes fixed on contour. Such membranes can be made from thin films pre-formed on silicon substrate after deep thorough etching of silicon from the wafer back side. The shape of area subject to etching defines the shape of the membrane contour. Diameter of the formed hole is several orders higher than membrane thickness. Membranes, made this way, are used, particularly in X-ray optics [1,2] and as sensing elements of sensors of various physical quantities [3–5], etc.

During calculations and design of MEMS-based devices it is necessary to use mathematical models, capable to forecast microstructure behavior under various physical and mechanical impacts. This mathematical tool is significantly different from the classical mechanics due to scale factors and is not completely developed yet. Therefore the development of mathematical models and their verification in accordance with experimental data are required. In this regard the current crucial task is a development of techniques of thin-film membranes parameters identification.

Analysis of membranes, fixed on contour, should be performed considering their geometrical dimensions and actual conditions of fixing, appearing during their manufacture. Significant impact of scale factor, particularly surface energy, change of effective properties, etc., appearing at sizes of several hundreds of nanometers — is noted in many studies [6–18]. Besides, the physico-mechanical aspects of manufacturing process (growth, etching, etc.) may have a great impact on specifics of residual stress distribution in thin-layer structures [19–21].

Classical equations of plates and shells theory do not consider this scale factor, therefore their application for evaluation of mechanical characteristics of thin-layer structures is not the best decision. Large amount of approximate methods for membranes voltage state evaluation at finite deformations are known, but usually they suggest a certain and rather simple deformation shape, for instance along spherical surface [22,23], that does not always correspond with experimental data. In this regard, it is preferable to use the approximate models, in which the effective properties are defined as per relatively simple formulas. Such approach is developed in this study.

This study is dedicated to description of experimentally observed features of membranes, formed above round

holes in silicon substrates, which are important for further analysis.

1. Membranes manufacturing

The studied membranes are single films or sets of films with overall thickness within the order of single micrometers and less, with diameter within the order of millimeter and less.

The studied membranes were manufactured [24] using technology based on Bosch-process of thorough etching of silicon substrates through masks formed on their back side. The specified process is highly selective to materials of membrane and mask and provides high anisotropy of silicon etching due to consecutive alternation of stages of reactive ion-plasma etching and plasma-chemical deposition by means of changing the composition of gaseous environment and voltage on a substrate holder. The example of the formed structure of four-layer membrane is presented in Fig. 1.

Non-uniformity of etching over the whole silicon wafer and necessity of polymer removal from deep holes result in higher time of over-etching. This results in membrane undercut and its thickness change along diameter.

After etching the film area above round hole becomes available, and this becomes the membrane. Due to presence of initial mechanical voltage in structure layers before etching [25–27] the non-zero initial deflection of the membrane [28–30] is observed. Actually, redistribution of internal forces results in additional deformations of membranes. As the same time, the increase of the film surface area in the membrane area happens.

Various etching profiles of the membrane bottom surface can be made depending on Bosch-process mode (Fig. 2) [24]. They influences the conditions of membrane fixing along support contour.

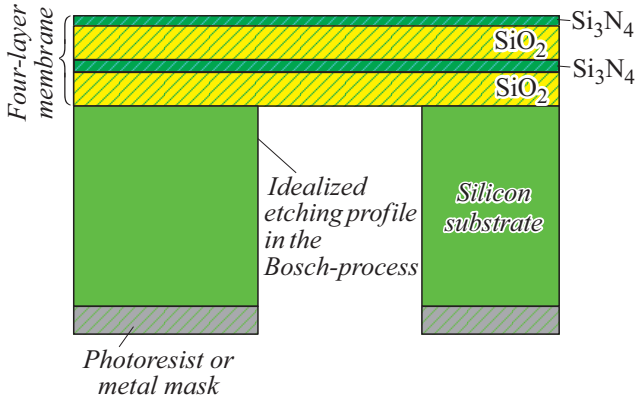

Figure 1. Formation of thin-film four-layer membranes on silicon substrate using Bosch-process

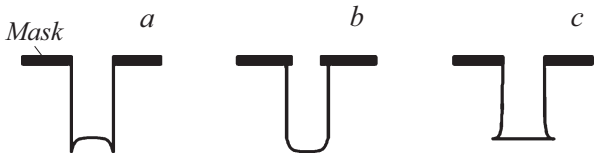

Figure 2. Various options of membranes bottom surface profiles depending on Bosch-process modes: *a* — profile with near-layer micro-trenching on bottom surface; *b* — profile with curved bottom surface; *c* — profile with side notching.

2. Membranes calculation and testing techniques. Defined parameters

Membranes behavior under overpressure, supplied from the side of the holes in silicon, was studied. The bench on a base of optical profilometer [2,31,32], performing the uniform supply and fixation of pressure value, as well as defining deflection of the membrane, was used for testing. Deflection means a small difference in height between membrane area and substrate area (membrane base), observed in the membrane center.

Due to wide popularity of plates and shells theory and simplicity of the equations proposed for calculation, they are often used for MEMS structures analysis [33–41]. For cases of deflection of fully-flexible membrane, characterized by the presence of stretching forces, radial displacement and elongation of middle plane:

$$\frac{Pa^4}{Eh} = \frac{7-\mu}{3(1-\mu)}\, w^3, \tag{1}$$

$$\frac{3.58w^3}{h^3} = \frac{Pa^4}{Eh^4} \quad (\text{at } \mu = 0.3), \tag{2}$$

where P — applied overpressure; a, h, μ, w, E — base radius, thickness, Poisson's ratio, deflection, Young's modulus of the membrane, respectively.

Another often used equation is the relation, obtained from suggestion on spherical shape of the membrane under overpressure [22,23]:

$$P = \frac{4\sigma_0 h}{a^2}\, w + \frac{8Eh}{3(1-\mu)a^4}\, w^3, \tag{3}$$

where σ_0 — mechanical voltage in the membrane without applied overpressure.

Is also used [41–45]

$$P = C_0 \frac{Eh^3}{(1-\mu)a^4}\, w + C_1 \frac{\sigma_0 h}{a^2}\, w + C_2 \frac{Eh}{(1-\mu)a^4}\, w^3, \tag{4}$$

where C_i — constant coefficients, selected empirically and dependent on structure geometry (for circular membranes they approximately equal to: $C_0 = 5.3$; $C_1 = 4.4$; $C_2 = 2.6{-}3.4$).

The technique of initial (residual [46–49]) mechanical voltage determination in a film on a substrate (without applied overpressure), also called as the Bubble method [50–52], should be additionally noted. In this case the round area

of the film, free from substrate, is created. With compression force the film will have initial deflection even without applied pressure, and the corresponding initial mechanical voltage can be defined in assumption of the spherical shape of the formed membrane considering equality of the potential deformation energy of the membrane U and external force energy A for movement, resulted by this deformation [53]:

$$\sigma_0 = \frac{E w_0^2}{(1-\mu)a^2}, \qquad (5)$$

where w_0 — membrane initial deflection.

However, on practice the initial membrane shapes are different — they can be convexed to different sides relative to fixing area, include both convex and concave areas (Fig. 3, *a*, 4, *a*, 5). Under overpressure the membrane can be analytically described with a spherical segment only approximately [22,23,27,30,54].

The membranes mechanical characteristics are defined considering the above mentioned equations or relations observed based on other approaches [36,54–65]. Thus, applied pressure P, membrane deflection w, base radius a and thickness h should be defined for membrane analysis.

3. Determination of initial dimensions and shape of membranes

Frequently the initial shape of membrane can be described with a flattened cone (Fig. 3, *a, b*). At manufacturing the membranes of various radius during single process the bigger radius membranes (Fig. 3, *a, b*) have almost flat lower base of the flattened cone, while smaller radius membranes (Fig. 3, *c, d*) have not.

Membrane shape change can also be caused by its location features during measurements. Particularly, when the membrane is located on holder at the bench in use [31], this holder is fixed on top and bottom, thus additionally pressing the membrane and making unidirectional creases (Fig. 4, *b, c*). Therefore the membrane shape and its pressing degree should be controlled [29]. It is important to distinguish the membrane creases caused by external exposure and creases caused by internal mechanical voltage of the released membrane (prone to radial symmetry).

The following was selected for observations over geometrical dimensions and shape of the membranes: optical profilometer Veeco Wyko NT 9300 and optical microscope Nikon Eclipse L200N. Optical profilometer was used for determination of membrane dimensions before and during testing, optical microscope — for initial screening. Using transmitted and reflected light, light and dark fields modes, the microscope allows to define diameters of the flattened cone bases, to control if the nontransparent silicon etched completely, to analyze defects, to evaluate nature of creases location, if present, etc. [66].

It can be assumed that the membrane radius is defined directly by photomask in use only. However, the hole diameter in the photomask can differ from actual observed membrane diameter. In Fig. 5, *a* the profile of surface of $SiN_x(0.13\,\mu m)/SiO_2(0.5\,\mu m)/SiN_x(0.13\,\mu m)/SiO_2(0.5\,\mu m)$ membrane is presented, hole radius of which was assumed equal to 0.5 mm, but actually was 0.57 mm. Since during calculation of elastic modulus E the value of the membrane radius base a is raised to the fourth power, this small deviation results in difference of more than by half.

Ellipsometry is conventionally used in microelectronics for transparent films thickness analysis [67–69]. The results of measurements of layers on a wafer before silicon etching from the back side are often used to define thickness, comprising the film membrane. However, at implementation of Bosch-process the membrane over-etching and its thickness change along diameter are possible. Therefore it is necessary to control the layers thickness directly on the membrane. Membranes of $p\text{-}Si^*(0.8\,\mu m)/SiN_x(0.13\,\mu m)/SiO_2(0.5\,\mu m)$ (estimated thickness is specified) of various diameter (hole diameters in the photomask are from 250 to 1000 μm), formed on the same wafer, were studied. It was observed that on all membranes the thickness of the bottom layer (SiO_2) is significantly lower (550 nm for membranes with diameter of less than 500 μm and 220−300 nm in the center for membranes with diameter of more than 500 μm), than on a crystal without membrane (650 nm). At the same time, on all membranes with diameter of more than 500 μm the thickness of SiO_2 layer closer to edge was 60−80 nm bigger, than in the center. By analyzing the same membranes using X-ray energy-dispersive microanalysis (EDX) [58,59], it was observed that on the membrane with diameter of less than 500 μm, the elemental oxygen (O) content in the center is higher, than closer to edge; on membranes with diameters of more than 500 μm the oxygen content in the center is lower than closer to edge. Thus, EDX data correspond to the results of spectral ellipsometry. It should also noted that at topography analysis of these membranes surface from the back side the reverse deflection was observed on membranes with diameter of more than 500 μm (Fig. 3, *b, d*). During these measurements the samples were freely located on a table. Measurements, performed at MicroProf200 unit, during which the sample did not contact the table in the area of membrane, showed the same surface shape.

This example shows that determination of shape and thickness of membranes is not a simple task: membrane shape is sophisticated and depends on many factors, membrane thickness is not uniform over its area, fixing conditions are varied.

4. Membrane fixing conditions influence

Another important aspect, influencing the voltage-strain state of membranes and limiting no-damage pressure (at increase of which the membrane destruction starts) — conditions of their fixing along support contour. Perfect fixing

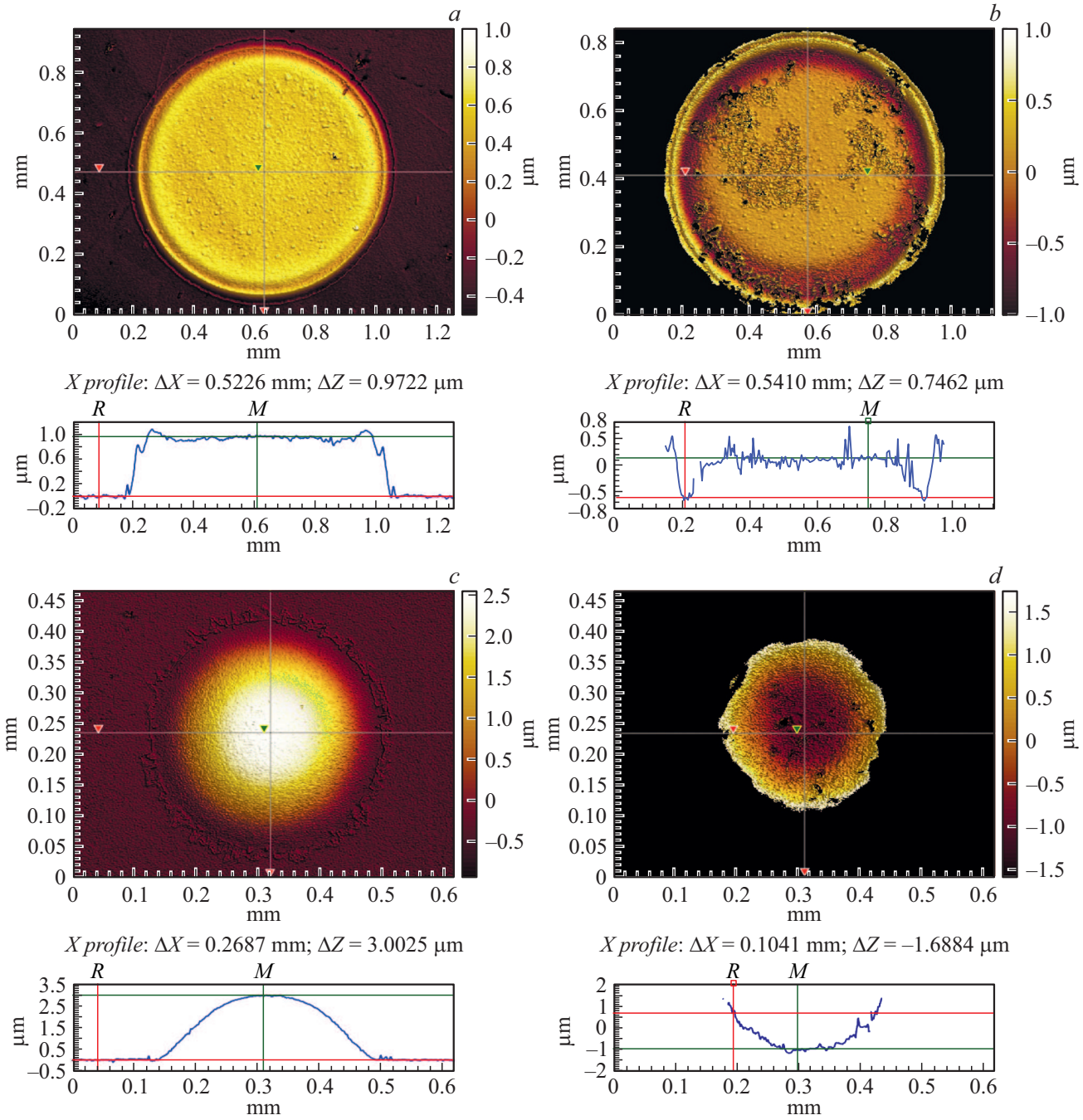

Figure 3. Topography and profiles of a surface of p-Si*/SiN$_x$/SiO$_2$ membranes: *a* — large diameter membrane, front view; *b* — large diameter membrane, back view; *c* — small diameter membrane, front view; *d* — small diameter membrane, back view.

models (hinged, rigid) are not capable to reflect the actual physico-mechanical parameters of support area, since during etching the materials properties and geometrical shape of support area surroundings are formed in sophisticated way (Fig. 2), can contain microcracks, etc.

Membrane destruction is often performed along its perimeter in the fixing area, the highest mechanical voltage is often observed along the membrane perimeter in the fixing area [2,33,39]. Therefore, the strengthening of the membranes fixing area by means of console reinforcements (supports) use is used as the method of these membranes reinforcement.

Since the analytical calculation of this type is complicated, the numerical modeling was performed. To evaluate the support parameters influence on membranes characteristics the parametric modeling was performed in COMSOL Multiphysics (software for mathematic modeling of physical processes, described with differential equations). Three-layer round membrane of Al($0.8\,\mu$m)/SiO$_2$($0.6\,\mu$m)/Al($1.1\,\mu$m) with base radius of $a = 750\,\mu$m [33] was deformed due

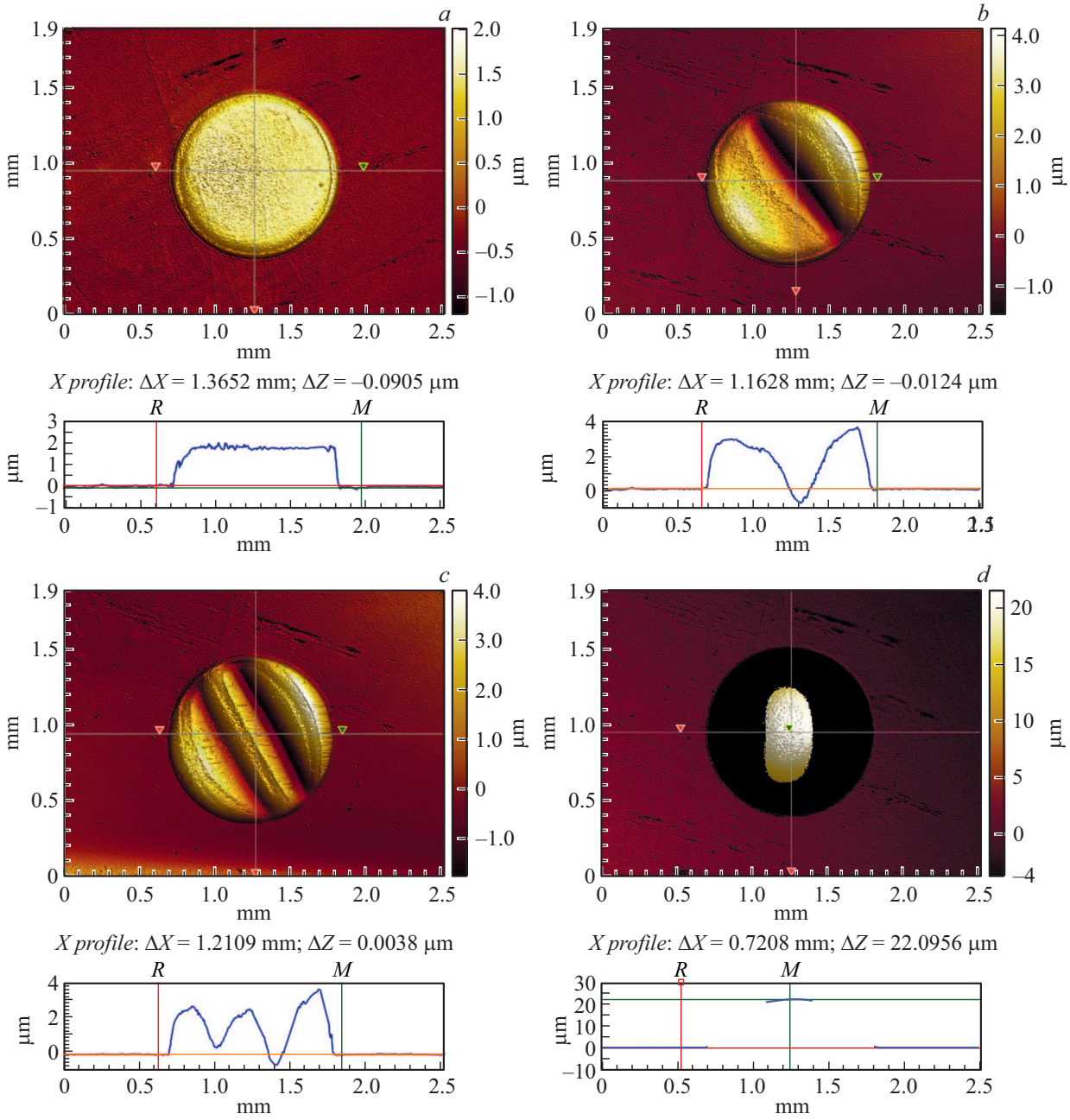

Figure 4. Topography and profiles of surface of p-Si*/SiN$_x$/SiO$_2$ membrane: a–c — change of membrane shape with increase of pressing degree; d — membrane shape at overpressure $P = 0.8$ atm.

to overpressure of $P = 0.3$ MPa. Membrane structure along it whole perimeter [70] was complemented with support of various materials: SiO_2 or Si. In section this ring support was of the form of rectangular triangle (Fig. 6, a).

Dependence of length, material and angle of support influence on membrane deflection, von Mises stress intensity [35,39], membrane shift from coordinate along radius are established (Fig. 6, b–d). The observed data correspond to the physical representations of membranes deformation.

Such numerical experiments are valued for selection of certain modes in practical applications. Also they can be used if it is necessary to obtain the membranes, withstanding the higher overpressure, or for determination of correcting (adjustment) coefficients during analysis of membranes with sophisticated fixing as per standard equations like (1)–(4).

5. Behavior of sophisticated shape membrane at overpressure supply

At overpressure increase the membrane shape gradually becomes closer to the spherical segment (Fig. 4, d). If the membrane is initially located above substrate level and similar to the flattened cone (Fig. 4, a), the cone gradually

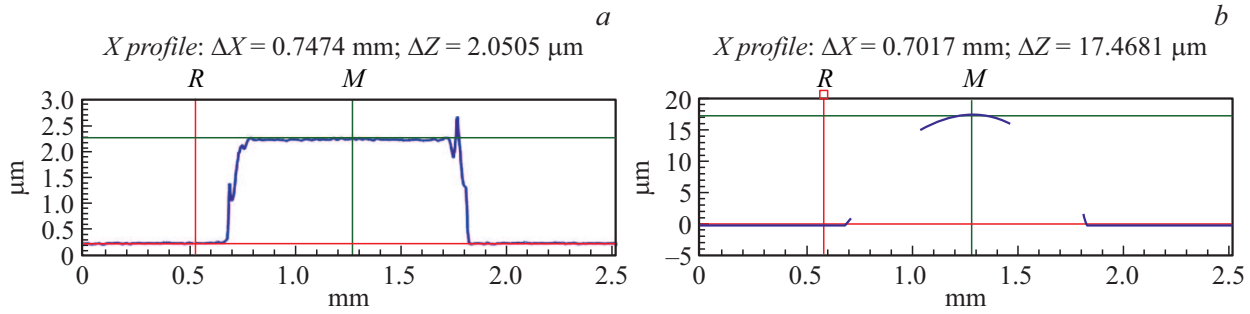

Figure 5. Profiles of surface of $SiN_x/SiO_2/SiN_x/SiO_2$ membrane: *a* — initial shape of membrane (before overpressure supply); *b* — membrane shape at overpressure $P = 0.4$ atm.

transitions to a shape similar to the spherical segment (Fig. 4, *d*). If the membrane has the sophisticated shape (Fig. 4, *b, c*), it also gradually becomes a convex cone. At the same time, the deflection value of the same membrane under its testing in case of various pressing degree at fixing (Fig. 4, *a*–*c*) is the same (Fig. 4, *d*). If the membrane was initially located below fixing area level (curved to another side), in the beginning it deflects little upwards, and then, starting from a certain pressure, sharply changes position and becomes closer to the spherical segment curved upwards, i.e. behaves like buckling membranes [62,63,71].

Many studies of analysis of deflection dependence on applied overpressure (diagrams, similar to Fig. 7) showed that these deformations can be considered elastic: several passes of gradual increase and decrease of pressure to membrane correspond to the same dependence diagram [31,32]. However, if pressure drops to zero, some membranes take original shape before overpressure supply, while others don't. The first case is probably related to presence of significant initial mechanical voltage in the membrane, (including the ones resulted by membrane fixing (Fig. 4)), that remained even after removal of overpressure and resulted in optimal membrane shape. The second case is supposedly observed in case of sufficiently free membranes, shape of which is defined by small disturbances.

Typically during membrane destruction it is completely detached from substrate [2,70,71], leaving the perfectly even hole (Fig. 8, *a*). However, in general case the various shapes of this hole are observed (Fig. 8).

6. Calculation of mechanical characteristics considering presence of initial deflection

Adaptation of the techniques for determination of mechanical characteristics ((1)–(4)) for membranes with initial deflection is of interest.

With increase of overpressure the membrane shape becomes similar to the spherical segment (Figs. 3, 5), which height (corresponding to the membrane deflection) is also gradually increasing. The area of membrane surface increases in similar way. Detailed accounting of actual membrane shape is complicated for analytical analysis. Change of membrane deflection in the area of elastic deformations with overpressure supply is important for determination of the membrane mechanical characteristics. Therefore, for the further calculations we will use the correspondence of actual area of membrane surface —area of model surface of the spherical segment. Thus, for analysis of membrane shape change from overpressure the change of membrane area or change of model spherical segment height can be used. For that it is necessary to calculate the initial area of membrane surface, and then to calculate the initial „effective deflection“ — height of model spherical segment.

In case of sufficiently simple membrane shape (Fig. 5, *a*), its surface area can be analytically calculated. For membrane shape similar to the flattened cone:

$$S = \pi \frac{d^2}{4} + \pi \sqrt{H^2 + \left(\frac{D}{2} - \frac{d}{2}\right)^2} \left(\frac{D}{2} + \frac{d}{2}\right), \qquad (6)$$

where S — membrane surface area, d — smaller base diameter, D — larger base diameter, H — height.

In case of more sophisticated surface shape, and in case of necessity to automate the changes, the calculation is performed numerically by means of application of triangular grid. Array of experimental data of surface topography is processed (X, Y, Z). For that it is necessary to define the area of membrane location [28] and summarize the elementary areas of all triangles — grid cells.

The corresponding „effective deflection“ w_{eff} of the membrane is calculated from the equation [29]:

$$w_{\text{eff}} = \sqrt{(S - S_0)/\pi}, \qquad (7)$$

where S — membrane surface area, S_0 — its base area, $S_0 = \pi a^2$.

At numerical calculation of the membrane surface area by means of the grid application the value of S_0 should also be calculated based on data array (X, Y, Z) and defined area of membrane location.

Equation (7) is applied only for circular membranes. However, its deriving for another shape of holes is performed the similar way.

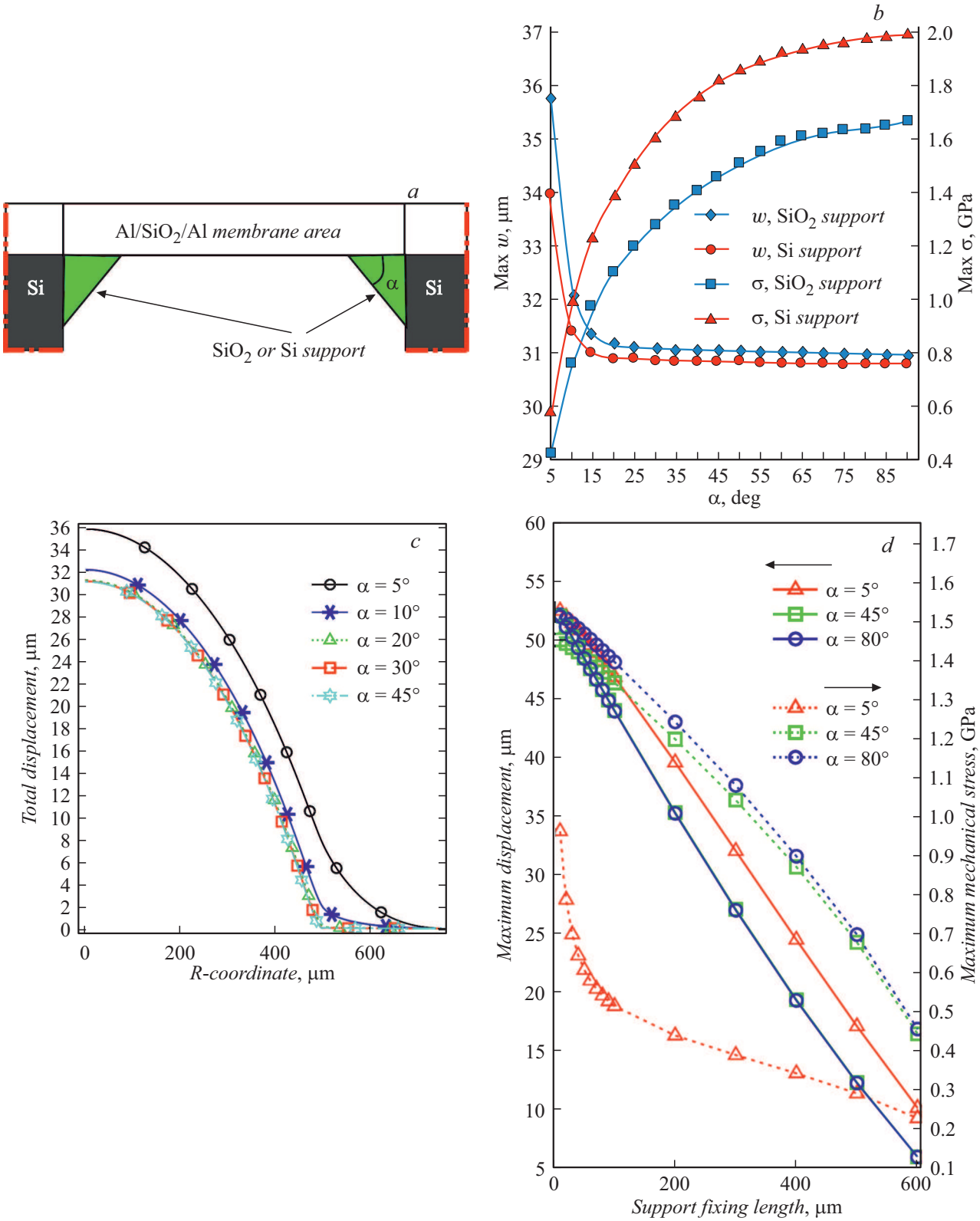

Figure 6. Support parameters influence on membrane behavior: *a* — schematic section image of $Al/SiO_2/Al$ membrane and support; *b* — dependence of maximum deflection and maximum von Mises stress intensity on the angle of support α and its material (for fixed contact length of 250 μm); *c* — value of membrane displacement from coordinate along radius for various angles of support (of SiO_2); *d* — dependence of maximum deflection and maximum von Mises stress intensity on the length of support and membrane contact (at fixed support angles of $\alpha = 5, 45, 80^\circ$).

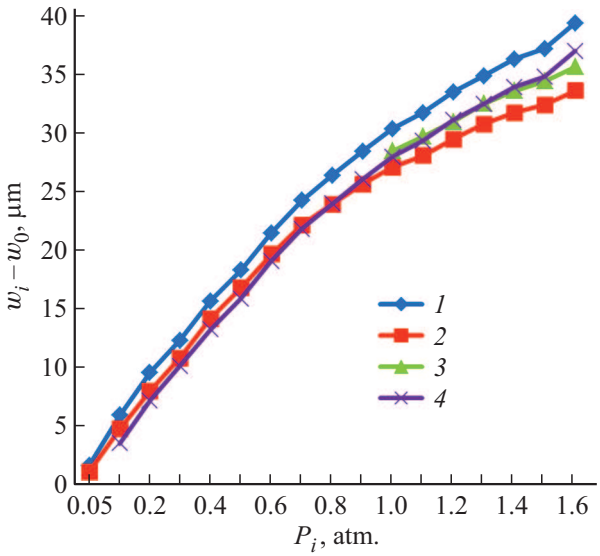

Figure 7. Dependence of deflection change $(w_i - w_0)$ on overpressure P_i for $SiN_x/SiO_2/SiN_x/SiO_2$ membrane: *1* (rhombuses) — w_0 and w_i are defined as per surface profiles, $w_0 = 2\,\mu$m; *2* (squares) — w_0 and w_i are calculated from (7), $w_0 = 4.3\,\mu$m; *3* (triangles) — w_0 and w_i are calculated from (7), missing data were defined as per author's technique, $w_0 = 4.3\,\mu$m; *4* (crosses) — w_0 is calculated from (7), w_i — are defined as per surface profiles, $w_0 = 4.3\,\mu$m.

During analysis the calculation of the „effective deflection“ of membrane with overpressure increase is performed. After the membrane shape becomes similar to the spherical segment, the value of the „effective deflection“ will be consistent with the measured one in terms of profile.

For analysis of dependence between membrane deflection and applied overpressure the difference between current membrane deflection w_i, if overpressure P_i exists, and initial „effective deflection“ w_0, if there is no applied overpressure, should be used (from the equation (7)). At the same time, the calculation of mechanical characteristics should be performed at non-linear section of $w(P)$ dependence near high pressure values.

Fig. 7 shows the dependence of deflection change $(w_i - w_0)$ with overpressure supply for $SiN_x(0.13\,\mu m)/SiO_2(0.5\,\mu m)/SiN_x(0.13\,\mu m)/SiO_2(0.5\,\mu m)$ membrane [29,32], the limiting no-damage pressure is 1.6 atm. Initial surface shape was a flattened cone with top base diameter of $d = 0.95$ mm, bottom base diameter of $D = 1.1431$ mm, height of $H = 2\,\mu$m (Fig. 5, *a*).

Initial „effective deflection“ defined from the surface area, was $4.42\,\mu$m at calculation using analytical equation (6) and $4.30\,\mu$m at calculation using triangular grid application. Considering accuracy of measurements and calculations the observed data are comparable.

Dependence, calculated as per method 2, shows the underestimated values of deflection near high pressure („squares“, Fig. 7). This is caused by limitations of the measurement method in use — lack of part of data on surface topography (Fig. 5, *b*). To calculate the membrane surface area the recovery of intermediate data using the embedded software is performed. However, at high pressure values there is also no data on the extreme edges of the membrane location, that complicates its shape recovery — instead of sharp transition (similar to Fig. 5, *b*) there is a smooth outgoing to the cone. Therefore, the data recovery program was developed, allowing to get the required membrane shape and then calculate w_i („triangles“, Fig. 7) on the assumption of such sharp transition.

Dependencies on Fig. 7, designated with triangles and crosses, almost coincide, that confirms the validity of the described technique and algorithms of calculation.

Let's give examples of calculation of effective elastic modulus of multi-layer membrane — value, corresponding to the complex of layers, comprising the membrane, and defined using equations (1)–(4), i.e. without express

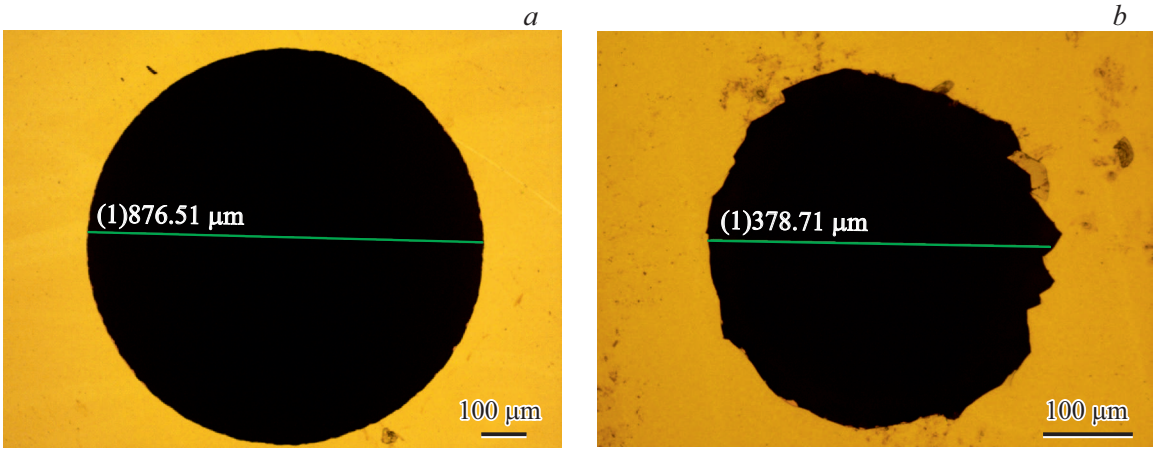

Figure 8. Image of holes, from optical microscope Nikon Eclipse L200N after membranes detachment: *a* — smooth hole (membrane testing from Fig. 3, *a, b*, separation at $P = 2.5$ atm); *b* — hole with ragged edges (membrane testing from Fig. 3, *c, d*, separation at $P = 4.5$ atm)

analytical accounting of features, caused by low thickness of structures. The equation [32,45] was used for determination of estimated elastic modulus of multi-layer structure:

$$E_{structure} = \frac{E_{layer1}h_{layer1} + \ldots + E_{layerN}h_{layerN}}{h_{layer1} + \ldots + h_{layerN}}. \quad (8)$$

For examined $SiN_x/SiO_2/SiN_x/SiO_2$ membrane $\mu = 0.214$ (since $\mu(SiO_2) = 0.2$, $\mu(SiN_x) = 0.27$), the calculation is similar to (8). As per (1) the effective elastic modulus of multi-layer membrane was $E = 110\,\text{GPa}$ (the calculation was performed at $P = 0.14\,\text{MPa}$, $w = (w_i - w_0) = 33.5\,\mu\text{m}$, $a = 0.57155\,\text{mm}$). The observed results is comparable with the estimated value of elastic modulus of this membrane as per (8). However, since the value of the initial deflection is low, its influence on numerical result of elastic modulus calculation is small [32].

The more indicative is the example of determination of the effective elastic modulus of multi-layer membrane for structure with significant initial deflection. Let's demonstrate the calculation using the example of the membrane of $Al(0.8\,\mu\text{m})/SiO_2(0.6\,\mu\text{m})/Al(1.1\,\mu\text{m})$ [29,32], the limiting no-damage pressure is 5.8 atm. $Al/SiO_2/Al$ membrane before overpressure supply had a shape close to the spherical segment, $w_0 = 30\,\mu\text{m}$, $a = 0.5264\,\text{mm}$. At $P_i = 0.24\,\text{MPa}$, $w_i = 60\,\mu\text{m}$, $w = (w_i - w_0) = 30\,\mu\text{m}$. Since $\mu(Al) = 0.34$, $\mu(SiO_2) = 0.2$, for this membrane $\mu = 0.3$. As per (2) the effective elastic modulus of multi-layer membrane was $E = 76\,\text{GPa}$. The observed result is comparable with the values of the elastic modulus for materials, comprising the membrane — aluminum and silicone oxide.

Thus, considering some above mentioned changes [29] the equations, similar to (1)–(4), can be used for analysis of membranes with initial deflection.

Conclusion

Experimentally observed features of the thin-film membranes, formed above round holes in silicon substrates, using Bosch-process of etching, are described. Specifics of this process, resulting in inexact match of the observed geometrical dimensions of membranes and conditions of fixing along the support contour — the estimated ones, are presented.

The necessity of exact determination of the membrane geometrical dimensions for correct calculation of mechanical characteristics by means of analysis of dependence of membrane deflection w from the supplied overpressure P is shown.

Membranes diameter was defined using optical profilometry and optical microscopy using the example of $SiN_x(0.13\,\mu\text{m})/SiO_2(0.5\,\mu\text{m})/SiN_x(0.13\,\mu\text{m})/SiO_2(0.5\,\mu\text{m})$ membranes.

Determination of the membrane transparent layers thickness using the example of $p\text{-}Si^*(0.8\,\mu\text{m})/SiN_x(0.13\,\mu\text{m})/SiO_2(0.5\,\mu\text{m})$ membranes (estimated thickness) with diameter of $250-1000\,\mu\text{m}$. According to spectral ellipsometry data the radial non-homogeneity of the bottom layer (SiO_2) thickness and thickness difference of this layer on membranes of various diameter are observed: for diameter of more than $500\,\mu\text{m}$ the thickness was $220-300\,\text{nm}$, in the center of membrane for diameter of less than $500\,\mu\text{m}$ the thickness was 550 nm, at crystal region without membrane — 650 nm.

It was shown that due to voltage state of the initial films, the actual shape of the formed membranes is not flat and not spherical segment. In many cases the membrane shape is similar to the flattened cone. Membrane shape is influenced by external exposure (location features during measurements).

Specifics of the membrane shape change during overpressure supply and its drop are described. With increase of the supplied pressure the membrane, that initially was similar to the flattened cone, like the more complicated membrane, gradually takes the shape similar to the spherical segment. Deformations are elastic.

By means of parametric modeling, using COMSOL Multiphysics, the dependences of length, material and support angle influence on behavior of $Al(0.8\,\mu\text{m})/SiO_2(0.6\,\mu\text{m})/Al(1.1\,\mu\text{m})$ membrane: its deflection, shift from coordinate along radius, von Mises stress intensity were established. The observed data correspond to the physical representations of membranes deformation.

In accordance with the developed technique of measurements and calculation of mechanical characteristics of the membranes, the effective elastic modulus of multi-layer structure of $SiN_x(0.13\,\mu\text{m})/SiO_2(0.5\,\mu\text{m})/SiN_x(0.13\,\mu\text{m})/SiO_2(0.5\,\mu\text{m})$ was 110 GPa, multi-layer structure of $Al(0.8\,\mu\text{m})/SiO_2(0.6\,\mu\text{m})/Al(1.1\,\mu\text{m})$ — 76 GPa.

The further studies assume consideration of thin-film membranes, described in this study, and use of the described techniques of their parameters identification for development of mathematical models of forecasting of the microstructures behavior under various physical and mechanical impacts.

Acknowledgements

The authors would like to thank E. Rzaev (AO „ZNTC“) for performing measurements using MicroProf200 and E.Yu. Yurasova (MIET) for performing the studies using X-ray energy-dispersive microanalysis method.

Funding

The study was performed by using equipment of the R&D Center of the „MEMSEC“ (MIET) with financial support of the Ministry of Science and Higher Education of the Russian Federation (№ 075-03-2020-216, 0719-2020-0017, mnemocode FSMR-2020-0017).

Conflict of interest

The authors declare that they have no conflict of interest.

References

[1] N.A. Djuzhev, M.A. Makhiboroda, R.Y. Preobrazhensky, G.D. Demin, E.E. Gusev, A.A. Dedkova. J. Surf. Investigation: X-ray, Synchrotron and Neutron Techniq., **11** (2), 443 (2017). DOI: 10.1134/S1027451017020239

[2] N.A. Djuzhev, E.E. Gusev, A.A. Dedkova, D.A. Tovarnov, M.A. Makhiboroda. Tech. Phys., **65**(11), 1755 (2020). DOI: 10.1134/S1063784220110055

[3] A. Nazarov, I. Abdulhalim. Sensors and Actuators A: Physical, **257**, 113 (2017). DOI: 10.1016/j.sna.2017.02.020

[4] C. Zorman. *Material Aspects of Micro- and Nanoelectromechanical Systems* (Springer Handbook of Nanotechnology, Springer-Verlag, Berlin 2007)

[5] N.A. Dyuzhev, E.E. Gusev, T.A. Gryazneva, A.A. Dedkova, D.A. Dronova, V.Yu. Kireev, E.P. Kirilenko, D.M. Migunov, D.V.Novikov, N.N. Patyukov, A.A. Presnukhina, A.D. Bakun, D.S. Ermakov, Nanotechnologies in Russia, **12** (7-8), 426 (2017). DOI: 10.1134/S1995078017040073

[6] P. Rosakis. Networks and Heterogeneous Media, **9** (3), 453 (2014). DOI: 10.3934/nhm.2014.9.453

[7] M. Kardar, G. Parisi, I.-Ch. Zhang. Phys. Rev. Lett., **56** (9), 889 (1986). DOI: 10.1103/PhysRevLett.56.889

[8] J. Braun, B. Schmidt. Calc. Var., **55** (5), 125 (2016). DOI: 10.1007/s00526-016-1048-x

[9] M.E. Gurtin, A.I. Murdoch. Archive for Rational Mechanics and Analysis, **57** (4), 291 (1975). DOI: 10.1007/bf00261375

[10] S. Majaniemi, T. AlaNissila, J. Krug. Phys. Rev. B, **53** (12), 8071 (1996).

[11] R. Molzon, C.S. Man. J. Elasticity, **20** (3), 181 (1988).

[12] B. Schmidt. Networks and Heterogeneous Media, **4** (4), 789 (2009).

[13] C.Q. Ru. Science China-Physics Mechanics & Astronomy, **53** (3), 536 (2010). DOI: 10.1007/s11433-010-0144-8

[14] C.Q. Ru. Continuum Mech. Thermodyn., **28** (1−2), 263 (2016). DOI: 10.1007/s00161-015-0422-9

[15] R. Shuttleworth. Proc. Phys. Soc. A, **63**, 444 (1950).

[16] F. Theil. ESAIM: M2AN, **45** (5), 873 (2011). DOI: 10.1051/m2an/2010106

[17] E. Orowan. Proc. Roy. Soc. Lond. A, **316**, 473 (1970).

[18] C.-Y. Hui, A. Jagota. Langmuir, **29** (36), 11310 (2013). DOI: 10.1021/la400937r

[19] S.A. Lychev, A.V. Manzhirov, T.N. Lycheva. Mechanics of Solids, **46** (2), 325 (2011). DOI: 10.3103/S002565441102021X

[20] S. Lychev, K. Koifman. Acta Mechan., **230** (11), 3989 (2019). DOI: 10.1007/s00707-019-02399-7

[21] S. Lychev. ZAMM Zeitschrift fur Angewandte Mathematik Mechanik, **94** (1−2), 118 (2014). DOI: 10.1002/zamm.201200231

[22] A. Degen, J. Voigt, B. Sossna, F. Shi, I.W. Rangelow. Proceedings SPIE, **3996**, 97 (2000).

[23] M.K. Small, W.D. Nix. J. Mater. Res., **7** (6), 1553 (1992).

[24] V.Yu. Kireev. *Nanotekhnologii v mikroelektronike. Nanolitografiya — protsessy i oborudovanie* (Izdatel'skiy dom „Intellekt“, Dolgoprudny, 2016) (in Russian).

[25] V.S. Sergeev, O.A. Kuznetsov, N.P. Zakharov, V.A. Letyagin. *Napryazheniya i deformacii v elementakh mikroskhem* (Radio i svyaz', M., 1987) (in Russian).

[26] G.P. Egorov. *Dissertatsiya na soiskanie uchenoy stepeni kandidata fiziko-matematicheskikh nauk „Mekhanicheskie napryazheniya v metallicheskikh plenkakh pri magnetronnom osazhdenii“* (NIYAU „MIFI“, M., 2018) (in Russian).

[27] S.F. Sen'ko, V.A. Zelenin. Pribory i metody izmereniy, **9** (3), 254 (2018). DOI: 10.21122/2220-9506-2018-9-3-254-262

[28] A.A. Dedkova, N.A. Dyuzhev, E.E. Gusev, M.Yu. Shtern. Rus. J. Nondestructive Testing, **56** (5), 452 (2020). DOI: 10.1134/S1061830920050046

[29] A.A. Dedkova, V.Yu. Kireev, V.A. Bespalov, A.L. Pereverzev. Patent RF 2758417 (in Russian).

[30] F.R. Brotzen. Intern. Mater. Rev., **39** (1), 24045 (1994).

[31] E.E. Gusev, A.A. Dedkova, N.A. Dyuzhev. Nanoindustriya, **S** (82), 538 (2018). DOI: 10.22184/1993-8578.2018.82.538.541

[32] A.A. Dedkova, E.E. Gusev, V.S. Larionov, N.A. Dyuzhev. Tretiy mezhdistsiplinarnyj molodezhnyj nauchnyj forum s mezhdunarodnym uchastiem „Novye materialy“. Sbornik materialov, 251 (2017) (in Russian).

[33] A.A. Dedkova, P.Yu. Glagolev, G.D. Demin, E.E. Gusev, P.A. Skvortsov. 2020 IEEE Conf. Rus. Young Researchers in Electrical and Electronic Engineering (EIConRus), 2288 (2020). DOI: 10.1109/EIConRus49466.2020.9039289

[34] E.I. Bromley, J.N. Randall, D.C. Flanders, R.W. Mountion. J. Vac. Sci. Technol. B, **1** (4), 1364 (1983).

[35] A.I. Kozlov. *Issledovanie i razrabotka membrannykh tenzopreobrazovateley davleniya. Dissertatsiya na soiskanie uchenoy stepeni kandidata tekhnicheskikh nauk.* (UlGTU, Ul'yanovsk, 2014), 113 s. (in Russian).

[36] N.M. Yakupov, V.N. Kupriyanov, R.G. Nurullin, S.N. Yakupov. Patent RF 2387973 (in Russian).

[37] J. Yang, W. Zhou, F. Yang. Patient CN101520385

[38] A.N. Gots. *Chislennye metody rascheta v energomashinostroenii. Uchebnoe posobie v dvukh chastyakh. Chast' 2* (Izd-vo Vladimirskogo gos. un-ta, Vladimir, 2010) (in Russian).

[39] L.E. Andreeva. *Uprugie elementy priborov* (Mashgiz, M., 1962) (in Russian).

[40] S.P. Timoshenko, S. Voynovsky-Kriger. *Plastinki i obolochki* (Nauka, M., 1966) (in Russian).

[41] A.A. Sachenkov. *Tsikl lektsiy po teorii plastin i obolochek: uchebnoe posobie* (Kazanskij universitet, Kazan, 2018) (in Russian).

[42] A.V. Korlyakov. Nano- i mikrosistemnaya tekhnika, **8**, 17 (2007) (in Russian).

[43] E.D. Khrebtova. *Razrabotka metodiki izmereniya mekhanicheskikh kharakteristik membrannykh elementov. Vypusknaya kvalifikatsionnaya rabota magistra po napravleniyu 28.04.01* (SPbGETU „LETI“, SPb, 2017), 99 s. (in Russian).

[44] I.A. Vavilin. *Razrabotka laboratornogo stenda dlya opredeleniya progiba mikromekhanicheskikh membran. Vypusknaya kvalifikatsionnaya rabota bakalavra po napravleniyu 28.03.01* (SPbGETU „LETI“, SPb, 2017) (in Russian).

[45] O.N. Astashenkova. *Fiziko-tekhnologicheskie osnovy upravleniya mekhanicheskimi napryazheniyami v tonkoplenochnykh kompozitsiyakh mikromekhaniki. Dissertatsiya na soiskanie uchenoy stepeni k.t.n. po special'nosti 05.27.06* (SPbGEU „LETI“, SPb, 2015), 143 s. (in Russian).
[46] I.A. Birger. *Ostatochnye napryazheniya* (Krasny pechatnik, L., 1963) (in Russian).
[47] P. Waters. Stress Analysis and Mechanical Characterization of Thin Films for Microelectronics and MEMS Applications. A dissertation submitted in partial fulfillment of the requirements for the degree of Doctor of Philosophy — 215 c., Department of Mechanical Engineering College of Engineering University of South Florida, 2008
[48] F. Fachin, S.A. Nikles, J. Dugundji, B.L. Wardle. J. Micromech. Microeng, **21**, 095017 (2011). DOI: 10.1088/0960-1317/21/9/095017
[49] A.N. Krivosheeva, A.V. Korlyakov, V.V. Luchinin, A.M. Efremenko. Patent RF 2327252 (in Russian).
[50] *Mekhanicheskie napryazheniya v tonkikh plenkakh* (*Referativno-analiticheskiy obzor*). Vypusk 8 (798). Seriya 2 „Poluprovodnikovye pribory“ (TsNII „Elektronika“, M., 1981) (in Russian).
[51] Pod red. L. Majsela, R. Glenga. *Tekhnologiya tonkikh plenok* (*spravochnik*) (Sov. radio, M., 1970) [Pers. s angl. M.I. Elinsona, G.G. Smolko, 1977] (in Russian)
[52] M.E. Galkina. Vnutrennie napryazheniya v uglerodnykh kondensatakh, formiruemykh impul'snym vakuumno-dugovym metodom. Dissertatsiya na soiskanie uchenoy stepeni k.f.-m.n., special'nost' 01.04.07 (Belgorodskij gos. un-t, Belgorod, 2005), 165 s. (in Russian).
[53] Electronic source. I. Karimov. „Lektsiya 4. Plastiny, membrany“ Available: http://www.soprotmat.ru/ lectuprugost4.htm (in Russian)
[54] G. Machado, D. Favier, G. Chagnon. Experimental Mechanics, **52**, 865 (2012). DOI: 10.1007/s11340-011-9571-3
[55] N.K. Galimov, S.N. Yakupov. Stroitel'naya mekhanika inzhenernykh konstruktsiy i sooruzheniy, **4**, 13 (2009) (in Russian).
[56] N.M. Yakupov, V.N. Kupriyanov, S.N. Yakupov. Izvestiya Kazanskogo gosudarstvennogo arkhitekturno-stroitel'nogo universiteta, **1** (9), 106 (2008) (in Russian).
[57] S.N. Yakupov. Izvestiya RAN. Mekhanika tverdogo tela, **3**, 58 (2011) (in Russian).
[58] N.M. Yakupov, S.N. Yakupov. Stroitel'naya mekhanika inzhenernykh konstruktsiy i sooruzheniy, **1**, 6 (2017) (in Russian).
[59] N.K. Galimov, S.N. Yakupov. Stroitel'naya mekhanika inzhenernykh konstruktsiy i sooruzheniy, **4**, 74 (2012) (in Russian).
[60] N.K. Galimov, S.N. Yakupov. Stroitel'naya mekhanika inzhenernykh konstruktsiy i sooruzheniy, **3**, 73 (2008) (in Russian).
[61] T. Tsakalakos. Metallurgical and Protective Coatings, **75**, 293 (1981).
[62] M.S. Ganeeva, V.E. Moiseeva, Z.V. Skvortsova. Uchenye zapiski Kazanskogo universiteta. Seriya fiziko-matematicheskie nauki, **160** (4), 670 (2018) (in Russian).
[63] I.P. Getman, M.I. Karyakin, G.O. Mostipan, I.A. Panfilov, Yu.A. Ustinov. Izvestiya vuzov. Severo-kavkazskiy region. Estestvennye nauki, **4**, 24 (2011) (in Russian).
[64] S. Jianbing, L. Xiang, X. Sufang, W. Wenjia. Interna. J. Polymer Sci., **2017**, 4183686 (2017). DOI: 10.1155/2017/4183686
[65] R.H. Plaut. Acta Mech., **202**, 79 (2009). DOI: 10.1007/s00707-008-0037-3
[66] A.A. Dedkova, M.A. Makhiboroda. Nanostruktury. Matematicheskaya fizika i modelirovanie, **20** (2), 41 (2020) (in Russian). DOI: 10.31145/2224-8412-2020-20-2-41-64
[67] V.A. Shvets, E.V. Spesivtsev, S.V. Rykhlitskii, N.N. Mikhailov. Nanotechnologies in Russia, **4** (3-4), 201 (2009). DOI: 10.1134/S1995078009030082
[68] Pod red. A. Zanderny. *Metody analiza poverkhnostey* (Mir, M., 1979) (in Russian)
[69] A.A. Dedkova, M.O. Nikiforov, S.V. Mitko, V.Yu. Kireev. Nanotechnologies in Russia, **14** (3-4), 176 (2019). DOI: 10.1134/S1995078019020046
[70] J.D. Baek, Y. Yoon, W. Lee, P. Su. Energy Environ. Sci., **8** (11), 3374 (2015). DOI: 10.1039/C5EE02328A
[71] N.E. Ol'khovsky. *Predokhranitel'nye membrany* (Khimiya, M., 1976) (in Russian).